**THE EUROPEAN**
**PHYSICAL JOURNAL**
**SPECIAL TOPICS**

Regular Article

# Protein transfer to membranes upon shape deformation

L.M.C. Sagis[1,2,a], E. Bijl[3], L. Antono[3], N.C.A. de Ruijter[4], and H. van Valenberg[3]

[1] Food Physics Group, Wageningen University, Bomenweg 2, 6703 HD Wageningen, The Netherlands
[2] Polymer Physics, Department of Materials, ETH Zurich, Wolfgang-Pauli-Str. 10, 8093 Zurich, Switzerland
[3] Dairy Science and Technology Group, Wageningen University, PO Box 8129, 6700 EV Wageningen, The Netherlands
[4] Wageningen Light Microscopy Centre, Laboratory of Cell Biology, Wageningen University, Droevendaalsesteeg 1, 6708 PB Wageningen, The Netherlands

**Abstract.** Red blood cells, milk fat droplets, or liposomes all have interfaces consisting of lipid membranes. These particles show significant shape deformations as a result of flow. Here we show that these shape deformations can induce adsorption of proteins to the membrane. Red blood cell deformability is an important factor in several diseases involving obstructions of the microcirculatory system, and deformation induced protein adsorption will alter the rigidity of their membranes. Deformation induced protein transfer will also affect adsorption of cells onto implant surfaces, and the performance of liposome based controlled release systems. Quantitative models describing this phenomenon in biomaterials do not exist. Using a simple quantitative model, we provide new insight in this phenomenon. We present data that show convincingly that for cells or droplets with diameters upwards of a few micrometers, shape deformations induce adsorption of proteins at their interface even at moderate flow rates.

## 1 Introduction

Cells, liposomes designed for controlled drug release, food based emulsions, or certain types of cosmetics and skin care products, are some typical examples of biomaterials with high surface to volume ratios. A better understanding of the complex dynamics of their phase interfaces, is highly relevant for a wide range of disciplines, which include biology, medical and pharmaceutical science, biophysics, material science, biotechnology, food science, coating technology, and chemical engineering [1]. One of the factors that makes the behavior of biomaterials with multiple phases so complex is the fact that mass and momentum transfer are coupled in these systems [1]. For example, mass transfer of water molecules across the interfaces affects the deformation of

[a] e-mail: `leonard.sagis@wur.nl`

phase-separated biopolymer droplets or vesicles in a flow field, leading to accelerated relaxation to a spherical shape after the flow is stopped [2–4]. Conversely, the high resistance against deformation of a gas-liquid interface, stabilized by crystallizing surfactants, can affect mass transfer of gas molecules across that interface, limiting the dissolution of microbubbles [5]. This coupling between deformation and mass transfer has been recognized as an important effect in geology [6], metallurgy [7–9], and solid state physics [10]. It has also been observed in bulk solutions of synthetic polymers [11], and suspensions of solid particles in a liquid phase [12]. In surfactant science it has long been recognized that deformations of an interface drive mass transfer of surfactants to and from the interface [1,13,14]. In contrast, in studies on the dynamic behavior of highly elastic membranes, deformation induced mass transfer between interface and bulk phase is in general not considered to be an important factor. The response of membranes to external flow fields is commonly attributed solely to in-plane interactions between the constituents of the membrane. Here we will show that this assumption is often not justified: we will show that flow induced deformations of elastic membranes can lead to irreversible adsorption of proteins to these membranes. This adsorption may alter their mechanical properties, such as their Young's modulus or bending rigidity, which has for example been documented for red blood cells [15–17]. For red blood cells their deformability is an important factor in platelet – vessel wall interactions [18], and in several diseases [19–21]. Protein adsorption induced by shape deformations is not accounted for in studies of protein adsorption on red blood cells [15–17].

In this paper we will present a quantitative model for describing the phenomenon, and present experimental data that show conclusively that this phenomenon is important for a wide range of systems, particularly when cells or droplets are larger than a few micrometers. We then discuss some particular examples of how this phenomenon affects complex biomaterials.

## 2 Deformation induced protein adsorption at elastic membranes

Flow induced adsorption should not be confused with the well-known Marangoni effect (or Gibbs-Marangoni effect), describing surface diffusion of adsorbed molecules as a result of in-plane gradients in surface concentration (in general also deformation induced). Deformation induced adsorption involves mass transport in directions perpendicular to the interface.

The mechanism for protein adsorption induced by shape deformations is as follows (Fig. 1A) consider a red blood cell in an arterial flow, or a fat droplet in milk being pumped through a pipe. The phospholipid membranes of these objects have an equilibrium surface tension of about $2\,\mathrm{mN/m}$. Pure proteins, when adsorbed at an interface tend to have equilibrium surface tensions in the range of $10$–$40\,\mathrm{mN/m}$, depending on the type of interface (water-oil, water-air) and protein concentration [1]. This means that in quiescent conditions proteins cannot adsorb at the membrane of a red blood cell or fat droplet, since this would lead to an increase of the surface tension, and therefore in an increase of the free energy of the system (Fig. 1B). Proteins will adsorb only when the surface tension of the membrane exceeds a threshold value, $\gamma_{th}$, equal to the equilibrium surface tension of the protein. When the threshold value is exceeded, adsorption of the protein lowers the free energy of the interface. The shape deformation of the cells or fat droplets induced by flow leads to an increase in their surface area ($\Delta A$), and in a decrease of the phospholipid concentration at their interface (Fig. 1C). This decrease in phospholipid surface concentration leads to an increase in the interfacial tension, given by [1,13,14]

$$\Delta\gamma = \gamma_d - \gamma_{nd} = E_d \Delta A/A \tag{1}$$
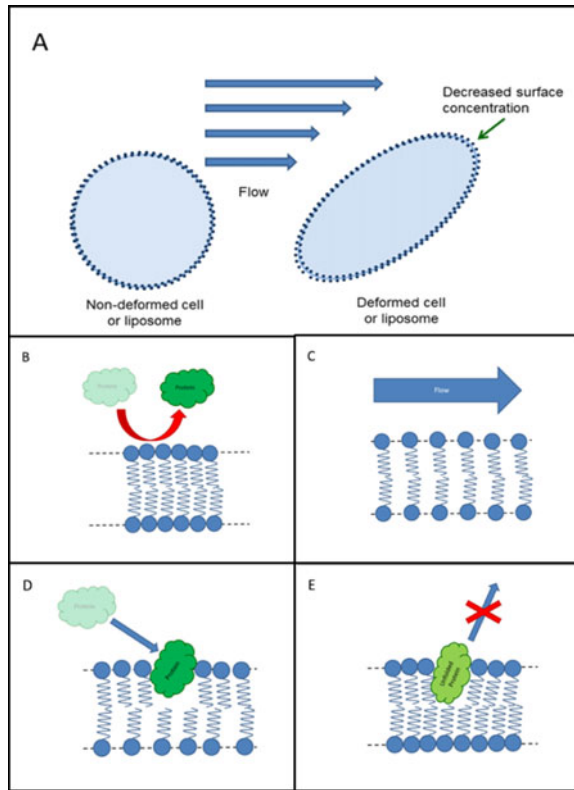
**Fig. 1.** Schematic representation of shape deformation induced adsorption of proteins on membranes. A) Liposome or cell is deformed in an arbitrary flow. B) In a non-deformed state the protein cannot adsorb to the membrane. C) The flow decreases the surface concentration of lipids, as a result the surface tension increases. D) As a result of increased surface tension proteins adsorb at the interface. E) If the protein unfolds, exposing its hydrophobic parts to the interior of the lipid bilayer, it will not desorb when the interface resumes a non-deformed state.

where $\gamma_{nd}$ is the surface tension of the non-deformed interface, $\gamma_d$ is the surface tension of the deformed interface, and $E_d$ is the dilatational modulus of the interface. When the mechanical forces are sufficiently strong, according to (1), the interfacial tension will increase above the threshold value $\gamma_{th}$, and protein will start to adsorb (Fig. 1D). Assuming that the actual adsorption to the interface is rate limiting (so we assume this process is much slower than diffusion/convection from the bulk phase to the immediate neighborhood of the interface), and assuming a linear relation between the protein flux towards the interface, $j_d$, and its driving force, we can express this flux as

$$j_d = k(T)(\gamma_d - \gamma_{nd}). \tag{2}$$

Here $k(T)$ is a transfer coefficient, which in a first approximation can be assumed to be a function of temperature, but not of concentration or degree of shape deformation. Equation (2) predicts a positive flux when $\gamma_d > \gamma_{th}$, indicating adsorption of protein, and a negative flux when $\gamma_d < \gamma_{th}$, indicating desorption of protein. When the droplet or cell relaxes to a non-deformed state, the surface tension decreases, and may attain values below $\gamma_{th}$. According to (2), the protein would then desorb again. However, in many cases proteins can unfold after adsorption to an interface, exposing the

hydrophobic parts of its structure towards the hydrophobic interior of the bilayer, and the hydrophobic interactions with the bilayer (or even the sub-phase, when this is a hydrophobic oil phase) will prevent the protein from desorbing (Fig. 1E). When sufficient amounts of protein remain adsorbed to the membrane, its rigidity will be altered significantly.

Here, for the sake of simplicity, we have used the concept of a dynamic (or transient) surface tension to describe the mechanism of deformation induced adsorption. Elsewhere in this issue we will discuss alternatives for this concept, which for elastic membranes may prove to be more suitable to describe the state of deformation of the membrane [22].

## 3 Materials and methods

Oil-in-water emulsions were prepared by premixing 4% (w/w) purified butter oil (VIVBuisman B.V.) with an aqueous solution of 0.5% (w/w) lecithin (L-$\alpha$-Phosphatidylcholine Type X-E, Sigma) in MilliQ water (Millipore Q-Gard 2). The premix was subsequently homogenized at 70 bar, for 10 min, in a Delta Instruments lab homogenizer. To these emulsions 10 U/mL FITC-labeled enzymes were added.

Lipoprotein lipase from bovine milk (0.62 mg/ml protein dissolved in 3.8 M ammonium sulphate, 0.02 M Tris-HCl buffer, pH 8, from Sigma) was labeled with FITC isomer 1 (Sigma) using a protocol described in reference [23]. A 2 mg/mL FITC solution in anhydrous dimethyl sulfoxide (DMSO) was prepared. Prior to addition of the FITC to the lipase solution, this solution was dialyzed against a 0.1 M sodium carbonate buffer of pH 9.05, overnight, at room temperature. The FITC solution was added as 5 $\mu$l aliquots to the protein solution, while being gently and continuously stirred. For each ml of protein solution, 35 $\mu$l of FITC solution was added. The final solution was stored in the dark, at room temperature for 5 hours. The excess FITC was removed by dialyzing against 0.1 M sodium carbonate buffer pH 8.5 for 2 days, during which the buffer solution was refreshed several times. Fluorescent FITC-labeled lipase has an extinction wavelength of 495 nm and emission wavelength of 525 nm (Sigma).

Emulsions were stirred for 6 hours by an overhead mechanical stirrer, at 20 °C, at 40 rpm or 150 rpm. It was not possible to use a non-stirred emulsion as a control, because as a result of the rather large droplet size, these emulsions show significant creaming in a time span of 6 hours. Coalescence events in the creamed layer could in principle lead to adsorption of lipase at the oil-water interface.

Droplet size distributions were determined using laser light diffraction with a Mastersizer 2000 (Malvern Instrument Ltd.). MilliQ water was used as a dispersant (refractive index 1.33). Settings chosen for the light scattering instrument are described elsewhere [24,25].

The distribution of FITC labeled lipase on oil droplets was analyzed using a LSM 510 META confocal microscope (Carl Zeiss). Samples were prepared by adding 10% (w/w) dextran (molecular weight equal to $2 \cdot 10^6$ Da, Sigma), to increase viscosity of the sample and thus reduce mobility of the oil droplets. Propyl-gallate (Sigma) was used as anti-fading agent. FITC-lipase was excited with 5% of the 488 nm line of a 30 mW Ar laser at 6.0 Amp and emission collected using a band pass filter with a range of 505–530 nm. Images were acquired with a 60× Plan Apo 1.4 NA objective and 1.1Airy Unit pinhole, thus collecting from 800 nm optical z-slices. Scan speed was 4 with detector gain at 1021 for all samples analyzed. Images were similarly processed in Adobe Photoshop by adapting the RBG settings to output 61- input 85 and output 199 and input 172. Since background intensity of the emulsion stirred at 40 rpm (Fig. 2 was lower (intensity 25) than in the other picture (intensity 40), this was corrected by adjusting the RBG default to output 118 and input 101, for correct comparison.
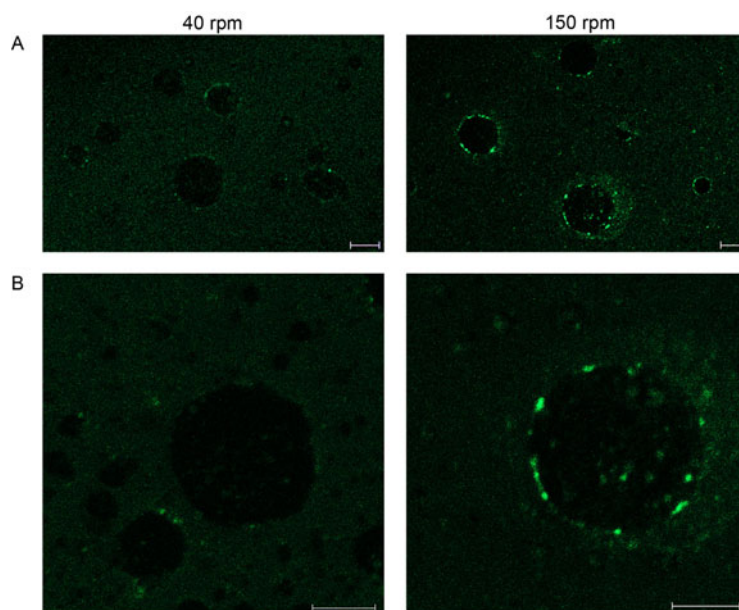
**Fig. 2.** A) CSLM images of samples stirred for 6 hours at 40 rpm (left) and 150 rpm (right) (scale bars equal 5 $\mu$m). At the highest stirring rate we clearly see adsorption of FITC labeled lipoprotein lipase at the interface of the droplets. B) Close-up of representative droplets at both stirring rates.

Interfacial tension and dilatational elastic modulus were measured with an oscillating drop tensiometer (Tracker, Teclis-IT Concept, Longessaigne, France). A drop of purified butter oil (VIVBuisman B.V., the Netherlands) was created at the tip of a u-shaped syringe, in an aqueous solution of 0.001% (w/w) phospholipids and 100 mM NaCl. The interfacial tension was determined from the drop profile by solving the Laplace equation. The equilibrium interfacial tension of the butter oil – phospholipid solution interface was found to equal $12 \pm 1$ mN/m. Injection of lipase into the aqueous phase under quiescent conditions did not affect this value. To determine if lipase can bind to the interface of a deformed oil droplet, the droplets were deformed using oscillatory deformations. The amplitude of oscillation was chosen in such a way that the maximum interfacial tension measured in each cycle was between 15 and 25 mN/m. The amplitude and period of deformation were 4 mm$^2$ and 30 s. Deformation was performed for five cycles (150 s) with interfacial tension measurement every 0.2 s, after which there was a period of 150 s in which the droplet area was not deformed, with measurements every 2 s. Each run lasted 14400 s. The first 3600 s the oil droplet - solution interface was allowed to reach its equilibrium interfacial tension. Next, oscillation of the drop was started, and after 7100 s lipase (200 units/280 $\mu$L of 3.8 M ammonium sulphate, 0.02 M Tris-HCl buffer at pH 8) or control (280 $\mu$l of the same buffer, without enzyme), was added to the aqueous phase. The elastic modulus was determined using expression (1), and its evolution after injection was monitored as a function of time.

## 4 Results and discussion

To illustrate deformation induced adsorption with experimental data we prepared a model emulsion from purified butter oil, stabilized by lecithin. FITC-labeled milk
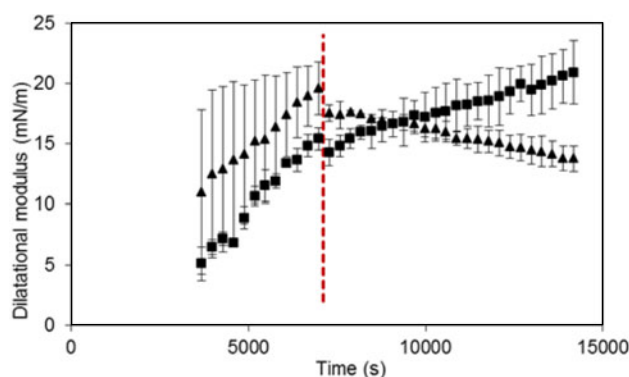
**Fig. 3.** Dilatational modulus $E_d$ as a function of time for a butter oil - phospholipid interface. Dashed red line marks the point where enzyme ($\triangle$) or enzyme-free buffer ($\square$) was injected into the aqueous phase (7100 s).

lipoprotein lipase was added to two samples of the emulsions and they were stirred at high speed (150 rpm), or low speed (40 rpm) respectively, using an overhead stirrer. Analysis of the particle size distribution showed that the stirring did not cause droplet break-up. Lipase interfacial binding was shown with CSLM (Fig. 2). In this figure we clearly see a more abundant fluorescent signal at the oil-water interface of the droplets in the sample stirred at 150 rpm. The fluorescent signal appears as irregularly spaced dots of variable size, that are more dense after high speed stirring (Fig. 2). At the lower stirring rate, significantly less adsorption of lipase can be detected. This clearly shows that lipase binding is controlled by the mechanical deformations of the droplets. The CSLM images were taken after stopping the flow, and the images show that the lipase adsorption was irreversible. Even droplets as small as about 5 $\mu$m in diameter show adsorption of the labeled lipase, indicating that this phenomenon is important for objects upwards of a few micrometers. This limit is of course affected by the rigidity of the original interface. Membranes with a higher rigidity require higher flow rates, or at equal flow rate, will show adsorption only for larger (and hence more deformable) objects.

Figure 3 shows the dilatational modulus of a butter oil - water interface stabilized by lecithin, determined by subjecting the interface to sinusoidal deformations in a drop tensiometer. The oscillation amplitude was equal to about 28.5%, a deformation sufficiently high to increase the surface tension of the interface from its equilibrium value ($12 \pm 1$ mN/m, see Materials and Methods) to a value above the threshold for protein adsorption. Note that this large amplitude induces a gradual increase in the dilatational modulus over time. At 7100 s either a lipase solution or an equal amount of lipase-free buffer was injected into the aqueous phase. When lipase is injected, adsorption of this protein leads to a significant decrease in the dilatational modulus, whereas the modulus of the other sample continues to increase in time. We see that this mode of adsorption can affect interfacial properties in a dramatic way.

Now that we have established the mechanism of shape deformation induced protein transfer, and have shown experimentally that for objects of a few microns in size it occurs already at moderate flow rates, we will discuss some of the effects of this type of adsorption for a number of systems. For cells the irreversible adsorption of sufficient amounts of proteins will affect the rigidity of the cell membrane [15–17]. For red blood cells their deformability is an important factor in the interaction between platelets and vessel walls [18], and in several diseases involving obstructions of the microcirculatory system [19–21]. Protein adsorption induced by shape deformations is not accounted for in studies of protein adsorption on red blood cells, in spite of

the fact that the cells are exposed to flow fields during these studies (either turbulent flows when stirring the samples, or shearing and extensional flows in microfluidics devices) [15–17]. Neglecting this effect may lead to errors in experimental data for protein adsorption coefficients and adsorption energies. To quantify the effect, studies should be performed not only at various protein and salt concentrations, but also at various flow rates.

Flow induced deformations can also affect the adsorption of cells onto surfaces of implants or artificial organs. Cell adsorption on implant materials plays a significant role in the development of infections that may occur after implantation, and these infections obstruct the long-term use of the materials [26, 27]. If deformations are sufficient to induce adsorption of charged proteins on the cell wall, the resulting change in surface charge of the cell wall can induce changes in the electrostatic interactions between surface and cell. Depending on the sign of the charges this may either reduce or increase cell adhesion. Shape deformation induced protein adsorption is not accounted for in studies of cell adhesion to solid walls, in spite of the fact that the phenomenon manifests itself already at relatively mild flow conditions.

Deformation induced adsorption will also be important in many pharmaceutical applications. The dynamic behavior of microcapsules used for controlled delivery is very sensitive to the mechanical properties of the capsule membrane [28]. Important parameters here are the membrane elasticity and its bending rigidity. These surface properties are a function of the composition of the interface, and will change when additional materials adsorb at the interface. The fact that these properties can change by deformation induced adsorption is in general not accounted for.

To illustrate how widespread this phenomenon is we discuss one final example: the effects of deformation induced protein adsorption in milk production. Automated robotic systems significantly reduce the workload for dairy farmers, and increase production per individual animal. They may however cause undesirable higher levels of free fatty acids (FFAs) in the milk [29]. FFAs cause an off odor and rancid taste, thereby reducing consumer appreciation of the milk. Plausible explanations for this effect have not yet been presented. The FFAs are produced by enzymatic hydrolysis of triglycerides present in the interior of the milk fat droplets, by the enzyme lipoprotein lipase. To react with the triglycerides, this water-soluble enzyme first has to adsorb to the oil-water interface of the fat droplets. This interface is a bilayer formed by phospholipids and proteins, and has an interfacial tension $<2\,\mathrm{mN/m}$ [29]. In view of this low tension, lipase cannot adsorb at the oil-water interface under quiescent conditions. Lipase could adsorb to the oil-water interface if this interface is disrupted by droplet break-up. However, although in an AMS forces exerted on the droplets are stronger than in regular milking systems, they are insufficiently strong to cause droplet break-up [30]. Wiking [30] showed that there was a significant increase in the free fatty acids content during pumping of 3.7% and 4% fat milk at $20\,^{\circ}\mathrm{C}$ and $31\,^{\circ}\mathrm{C}$ when the shear rate was increased from $172\,\mathrm{s}^{-1}$ to $565\,\mathrm{s}^{-1}$, even though no significant break-up of the oil droplets occurred. Our experiments suggest that the rancidity is caused by deformation induced transfer of lipase to the membrane of the milk fat droplets. While pumping the milk through the lines of the milk robot, fat droplets are deformed, and this allows the lipase to adsorb at the droplet membrane (similar to what we see in Fig. 2). After adsorption it starts to hydrolyze the triglycerides in the interior of the droplet, and the FFAs produced in this process are transferred in part to the aqueous phase of the milk, producing a rancid taste. To establish whether deformation induced protein adsorption is indeed responsible for the FFA production, we need to determine if the flow conditions in AMS systems are sufficient to induce this phenomenon. Lipase can adsorb at oil-water interfaces when the surface tension exceeds a certain threshold value. This value may vary significantly between different variants of this protein. Flipsen [31] showed that variants of cutinase, which is a lipase,

could have an equilibrium surface tension at the oil-water interface with a difference of about 22 mN/m. The highest equilibrium surface tension found was 23.8 mN/m for an inactive variant, and the lowest was 1.7 mN/m. For the sake of convenience we will assume a value of 12 mN/m for our threshold for lipase adsorption (roughly in the middle of this range). With a value of 2 mN/m for the lipid bilayer surface tension this gives us a value for $\Delta\gamma$ equal to 10 mN/m, for adsorption of lipase to occur as a result of deformation. A typical value for $E_d$ of phospholipid bilayers is about 100 mN/m [32], and with equation (1) this value allows us to calculate the relative change in surface area needed to reach the threshold value for adsorption. If we assume the droplets are deformed to a prolate ellipsoidal shape, their degree of deformation can be characterized by the parameter $d = (l - b)/(l + b)$, where $l$ and $b$ are the lengths of the long and short axis of the ellipsoid. For a given value of $d$, the increase of the surface area of the droplet equals [33]

$$\frac{\Delta A}{A} = \frac{1}{2}q^{2/3}\left(1 + \frac{w}{q^2 \tan w}\right) - 1 \tag{3}$$

where $q = (1 - d)/(1 + d)$, and $w = \arccos(q)$. From Eqs. (1) and (3) we find that for a lipid bilayer with equilibrium interfacial tension equal to 2 mN/m, and a dilatational modulus of 100 mN/m, a deformation $d = 0.38$ is sufficient for $\gamma_d$ to reach a threshold value of 12 mN/m. We now need to link this deformation to the typical flow conditions in an AMS. The degree of deformation of the droplets depends on the capillary number $Ca$, the viscosity ratio $\lambda$ (oil phase viscosity divided by aqueous phase viscosity), and the type of flow (shear, elongation, turbulent flow). Here we will assume that the flow in the system is an isotropic turbulent flow, with energy dissipation per unit mass equal to $\varepsilon$. Closed form relations expressing $d$ in terms of $Ca$ and $\lambda$ for this type of flow do not exist, and $d$ has to be determined numerically [34]. Closed form relations do however exist for shear and elongation flow. For shear flow $d$ is related to $Ca$ and $\lambda$ by the familiar Taylor expression [35,36]

$$d = Ca\frac{19\lambda + 16}{16\lambda + 16}. \tag{4}$$

Since shear is less efficient to deform droplets than elongation or turbulent flow, using Eq. (4) overestimates the value for $Ca$, needed to reach the threshold value for $\gamma_d$. This is particularly true for systems with large viscosity ratios, such as in our system. Moreover, (4) is valid only in the limit of small deformations. So, here we use this simple expression only as a rough estimate of the upper bound, above which we may definitely expect lipase adsorption to occur. More accurate relations linking droplet deformation to the capillary number can be found in the literature [34]. The viscosity ratio of our system is equal to 75, and using (4) we find that to reach a value for $d$ equal to 0.38, we need a capillary number of 0.32.

We must now relate the capillary number to the characteristics of the flow in AMS. From the energy dissipation we can calculate the Kolmogorov length scale, given by [37]

$$l_K = (\mu/\rho)^{3/4}\varepsilon^{-1/4} \tag{5}$$

where $\rho$ is the density of the continuous phase, and $\mu$ is the shear viscosity of the continuous phase. For typical values for the viscosity ($10^{-3}$ Pa s) and density ($10^3$ kg/m$^3$), an energy dissipation of 100 J/(kg s) results in a Kolmogorov length scale of about $10\,\mu$m. The oil droplets in milk have a volume-surface averaged diameter of about $4\,\mu$m [38]. The larger droplets of the size distribution have a diameter above $10\,\mu$m [38], and are larger than the Kolmogorov length scale. These droplets are most easily deformed and therefore most likely to show lipase adsorption. We will therefore use these larger droplets to estimate the energy dissipation for which the
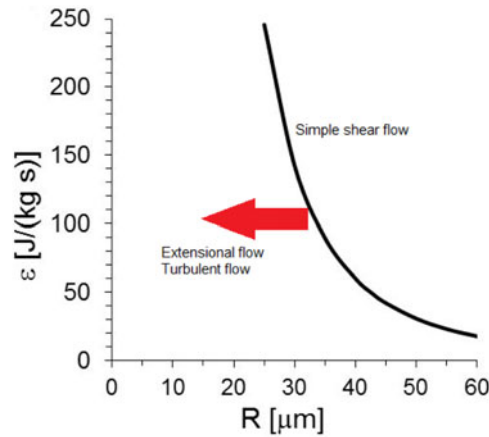
**Fig. 4.** Energy dissipation $\varepsilon$ [J/(kg s)] needed to induce deformation induced protein adsorption, as a function of the radius of the droplet $R$. The solid line was calculated using an expression for the deformation of the droplet, valid for a simple shear flow. For extensional or turbulent flows we would expect this curve to shift to the left, as indicated by the red arrow.

threshold value will be reached. Since the droplet size is of the same order or larger than the Kolmogorov scale, these droplets are in the inertial deformation regime, and the capillary number is given by [39]

$$Ca = \frac{R^3 \rho^2 \varepsilon}{\mu \gamma_d}. \tag{6}$$

With this expression we can estimate the energy dissipation per unit mass needed to reach a threshold value for the surface tension of 12 mN/m. Equation (6) shows us that the energy dissipation needed to reach the threshold scales with droplet radius as $R^{-3}$ (see also Fig. 4). This shows that the smaller droplets in the size distribution need energy inputs to reach the threshold surface tension far in excess of those encountered in an AMS, and we may indeed expect only the larger droplets to show lipase adsorption. In Fig. 4 we have plotted the upper bound for the energy input needed to induce lipase adsorption as a function of droplet size. If we assume that in an AMS milk is being pumped through a pipe with diameter $D$, at a flow rate $Q$, than the rate of energy dissipation scales as $\varepsilon \sim Q^3 D^{-7}$ [40]. At a flow rate of the order of 0.1 m$^3$/s, and a pipe diameter of the order of 0.01 m, we would expect a rate of energy dissipation in the system of the order of 100 J/(kg s). In Fig. 4 we see that droplets with a radius of about 30 $\mu$m would be deformed sufficiently to allow lipase adsorption. Although the majority of droplets in milk is smaller than this value [38], such droplets can be found in milk. As pointed out before, our model calculates only a rough estimate of the droplet size above which lipase adsorption could be observed, using an expression for the deformation $d$ valid only for simple shear flow [see equation (4)]. In an actual AMS the flow would be turbulent, and for this type of flow we would expect the curve in Fig. 4 to shift to the left, as indicated by the red arrow. So in turbulent flow fields the size of the affected droplets would be significantly smaller than 30 $\mu$m, which is also confirmed by our results depicted in Fig. 2, where droplets as small as 5 $\mu$m show lipase adsorption. Our analysis shows that it is highly plausible that deformation induced protein adsorption is responsible for the FFA production in automated milking systems. The mechanism we have proposed here suggests

a simple solution for the problem: reducing the flow rate should decrease the degree of deformation of the fat droplets, thereby decreasing the amount of adsorbed lipase.

## 5 Conclusions

The examples of protein adsorption to membranes induced by shape deformations we discussed in this article clearly illustrate the importance of this phenomenon in the dynamics of a wide range of biomaterials, such as cells, liposomes, or food based emulsions. We have discussed its role in systems such as red blood cells in arterial flows, and in milk produced with milking robots. When modeling the dynamics of such systems it may often not be sufficient to model the in-plane rheology of the interfaces by a constitutive model with constant material properties. We will need to account for the fact that the momentum and mass balances describing the state of the interface may be coupled: deformation of the interface may induce mass transfer of components between the bulk phase and the interface, and the resulting change in material properties will in turn affect the deformation of the interface. The model we presented here is a relative simple phenomenological model, but yet provides remarkable insight in the mechanism. A more rigorous approach to incorporating this effect in the description of the dynamics of multiphase biomaterials can be constructed within the framework of nonequilibrium thermodynamics [1,41,42].

## References

1. L.M.C. Sagis, Rev. Mod. Phys. **83**, 1367 (2011)
2. E. Scholten, J. Sprakel, L.M.C. Sagis, E. van der Linden, Biomacromolecule **7**, 339 (2006)
3. E. Scholten, L.M.C. Sagis, E. van der Linden, J. Phys. Chem. B **110**, 3250 (2006)
4. L.M.C. Sagis, J. Controlled Release **131**, 5 (2008)
5. E. Dressaire, R. Bee, D.C. Bell, A. Lips, H.A. Stone, Science **320**, 1198 (2008)
6. D.R. Lentz, Can. Mineral **37**, 489 (1999)
7. T. Kajitani, J. Drezet, M. Rappaz, Metall. Mater. Trans. A **32A**, 1479 (2001)
8. E.P. Elsukov, I.V. Povstugar, A.L. Ul'yanov, Phys. Metals Metallogr. **107**, 80 (2009)
9. V.A. Shabashov, V.V. Sagaradze, A.V. Litvinov, Mat. Sci. Eng. A **528**, 6393 (2011)
10. K. Detemple, O. Kanert, K.L. Murty, J.T.M. De Hosson, Phys. Rev. B **44**, 1988 (1991)
11. M. Tirrell, M.F. Malone, J. Polym. Sci. **15**, 1569 (1977)
12. J. Mewis, N. Wagner, *Colloidal Suspension Rheology* (Cambridge University Press, Cambridge, 2002)
13. B. Levich, *Physicochemical Hydrodynamics* (Prentice Hall, Englewoods Cliffs NJ, 1962)
14. J. Lucassen, M. van den Tempel, J. Colloid Interface Sci. **41**, 491 (1972)
15. Y. Kikuchi, T. Koyama, Am. J. Physiol. **247**, H739 (1984)
16. Y. Kikuchi, T. Koyama, Am. J. Physiol. **247**, H748 (1984)
17. M. Paulitschke, G.B. Nash, D.J. Anstee, M.J.A. Tanner, W.B. Gratzer, Blood **86**, 342 (1995)
18. P.A. Aarts, R.M. Heethaar, J.J. Sixma, Blood **64**, 1228 (1984)
19. O. K. Baskurt, D. Gelmont, H.J. Meiselman, Am. J. Respir. Crit. Care Med. **157**, 421 (1998)
20. A.M. Dondorp, B.J. Angus, K. Chotivanich, K. Silamut, R. Ruangveerayuth, M.R. Hardeman, P.A. Kager, J. Vreeken, N.J. White, Am. J. Trop. Med. Hyg. **60**, 733 (1999)

21. A.M. Dondorp, P.A. Kager, J. Vreeken, N.J. White, Parasitol. Today **16**, 228 (2000)
22. L.M.C. Sagis, Eur. Phys. J. Special Topics **222**, 39 (2013)
23. B.N. Dardik, C.D. Schwartzkopf, D.E. Stevens, R.E. Chatelain, J. Lipid Research **41**, 1013 (2000)
24. M.C. Michalski, V. Briard, F. Michel, Lait **81**, 787 (2001)
25. J.A. O'Mahony, M.A.E. Auty, P.L.H. McSweeney, J. Dairy Res. **72**, 338 (2005)
26. C. Von Eiff, G. Peters, C. Heilmann, Lancet Infect. Dis. **2**, 677 (2002)
27. J. Vincent, Lancet **361**, 2068 (2003)
28. D. Barthès-Biesel, J.M. Rallison, J. Fluid Mech. **113**, 251 (1981)
29. L. Wiking, L. Bjorck, J.H. Nielsen, Int. Dairy J. **13**, 797 (2003)
30. L. Wiking, J.H. Nielsen, A.K. Bavius, A. Edvardsson, K. Svennersten-Sjaunja, J. Dairy Sci. **89**, 1004 (2006)
31. J.A.C. Flipsen, M.A. van Schaick, R. Dijkman, H.T.W.M. van der Hijden, H.M. Verheij, M.R. Egmond, Chem. Phys. Lipids **97**, 181 (1999)
32. R. Kwok, E.A. Evans, Biophys. J. **35**, 637 (1981)
33. W.H. Beyer, *CRC Standard Mathematical Tables*, 28th edn. (CRC Press, Boca Raton FL, 1987)
34. P.L. Maffettone, M. Minale, J. Non-Newtonian Fluid Mech. **78**, 227 (1998)
35. G.I. Taylor, Proc. R. Soc. A **138**, 41 (1932)
36. G.I. Taylor, Proc. R. Soc. A **146**, 501 (1934)
37. M.T. Landahl, E. Mollo-Christensen, *Turbulence and Random Processes in Fluid Mechanics*, 2nd edn. (Cambridge University Press, Cambridge, 1992)
38. P. Walstra, J.T.M. Wouters, T.J. Geurts, *Dairy Science and Technology*, 2nd edn. (CRC Press/Taylor and Francis, Boca Raton FL, 2005)
39. V. Cristini, J. Blawzdziewicz, M. Loewenberg, L.R. Collins, J. Fluid Mech. **494**, 231 (2003)
40. G.A. Hughmark, Ind. Eng. Chem. Fundam. **16**, 307 (1977)
41. D.A. Edwards, H. Brenner, D.T. Wasan, *Interfacial Transport Phenomena and Rheology* (Butterworth-Henemann, Boston, 1991)
42. J.C. Slattery, L.M.C. Sagis, E.S. Oh, *Interfacial Transport Phenomena*, 2nd edn. (Springer, New York, 2007)